Virus Research, 1 (1984) 153–167
Elsevier

VRR 00112

Replication and morphogenesis of avian coronavirus in Vero cells and their inhibition by monensin

Firelli V. Alonso-Caplen *, Yumiko Matsuoka, Graham E. Wilcox ** and Richard W. Compans

Department of Microbiology, University of Alabama in Birmingham, Birmingham, AL 35294, U.S.A.

(Accepted 12 January 1984)

Summary

Avian infectious bronchitis virus (IBV) was adapted to Vero cells by serial passage. No significant inhibition of IBV replication was observed when infected Vero cells were treated with α-amanitin or actinomycin D. In thin sections of infected cells, assembly of IBV was observed at the rough endoplasmic reticulum (RER), and mature IBV particles were located in dilated cisternae of the RER as well as in smooth cytoplasmic vesicles. In addition to typical IBV particles, enveloped particles containing numerous ribosomes were identified at later times postinfection. Monensin, a sodium ionophore which blocks glycoprotein transport to plasma membranes at the level of the Golgi complex, was found to inhibit the formation of infectious IBV. In thin sections of infected Vero cells treated with the ionophore, IBV particles were located in dilated cytoplasmic vesicles, but fewer particles were found when compared to controls. A similar pattern of virus-specific proteins was detected in control or monensin-treated IBV-infected cells, which included two glycoproteins (170000 and 24000 daltons) and a polypeptide of 52000 daltons. These results suggest that the ionophore inhibits assembly of a virus which matures at intracellular membranes.

Key words: avian coronavirus, IBV replication, IBV morphogenesis, monensin

* *Present address*: Virology Division, USAMRIID, Fort Detrick, Frederick, MD 21701, U.S.A.
** *Permanent address*: School of Veterinary Studies, Murdoch University, Murdoch, Western Australia.

Introduction

Infectious bronchitis virus (IBV), the prototype avian coronavirus, is an enveloped virus which contains a large single-stranded RNA genome of positive polarity (Schochetman et al., 1977; Robb and Bond, 1979; Siddell et al., 1983). IBV virions exhibit moderate pleomorphism, and bear club-shaped surface projections about 20 nm in length which are characteristically widely-spaced (Robb and Bond, 1979). Although there has been considerable variation in the structural polypeptides reported for coronaviruses, three classes of polypeptides are generally found including a nucleoprotein (50–60 000 daltons), a membrane-associated glycopolypeptide (20–35 000 daltons) and a high mol. wt. glycoprotein that constitutes the surface projections (Siddell et al., 1982).

Monensin, an ionophore which preferentially transports sodium ions across membranes, was previously reported to inhibit the release of secretory glycoproteins and the appearance on the cell surface of membrane glycoproteins (Tartakoff and Vassalli, 1977, 1978; Ledger et al., 1980; Tajiri et al., 1980). The replication and glycoprotein transport of several enveloped viruses were reported to be inhibited by monensin (Johnson and Schlesinger, 1980; Johnson and Spear, 1982; Madoff and Lenard, 1982; Srinivas et al., 1982). We have obtained evidence that this ionophore selectively blocks VSV replication and the transport of its membrane glycoprotein to Madin–Darby canine kidney (MDCK) cell surfaces, whereas assembly and glycoprotein transport of influenza viruses are unaffected in these cells (Alonso and Compans, 1981; Alonso-Caplen and Compans, 1983). Unlike most other enveloped RNA viruses which bud from plasma membranes of infected cells, IBV particles assemble at the intracellular membranes of the rough endoplasmic reticulum (RER) (Becker et al., 1967). It was therefore of interest to determine the effects of monensin on IBV replication. We have investigated the effects of the ionophore on replication, polypeptide synthesis, and morphogenesis of IBV in Vero cells, a continuous cell line of African green monkey kidney origin. The results indicate that monensin affects assembly of this virus, which is not known to direct its membrane glycoproteins through the Golgi apparatus.

Materials and Methods

Viruses and cells

The Beaudette strain of IBV was obtained from the American Type Culture Collection (ATCC). The virus was initially grown in primary chick kidney cells, passaged twice in 10-day-old chicken embryos, and then adapted to Vero (ATCC) cells by a series of 'blind' passages at 24 h intervals. After the tenth passage in Vero cells, cytopathic effects were observed including syncytium formation and rounding up of cells eventually leading to detachment from their substratum. Virus stocks were prepared after the tenth passage by infecting confluent monolayers of Vero cells. After a 90 min adsorption period, serum-free Dulbecco's modified Eagle's medium (DMEM) was added and viruses were harvested at 24 h postinfection.

Stocks of influenza A virus (WSN strain) were prepared on Madin–Darby bovine kidney (MDBK) cells (Choppin, 1969) and VSV stocks (Indiana strain) were obtained in BHK21 cells (Roth and Compans, 1980). MDCK, BHK21, and MDBK cells were grown by described procedures (Holmes and Choppin, 1966; Roth and Compans, 1980). Vero cells were maintained in DMEM containing 10% newborn calf serum. All cells were grown at 37°C in an atmosphere of 5% CO_2 in air.

Plaque assay

IBV infectivity titers were measured by plaque assays on confluent monolayers of Vero cells in 35 mm tissue culture dishes. The monolayers were washed twice with phosphate-buffered saline, pH 7.2 (PBS), and inoculated with 0.2 ml of serial dilutions of IBV. After an adsorption period of 2 h at 37°C, the cells were washed once with PBS, and 4 ml of overlay medium (0.6% agarose in serum-free DMEM) was added. Plaques, usually ranging from 0.5 to 3.0 mm in diameter, started to appear 2 days postinfection. At 3–4 days after infection, cells were stained by the addition of a second overlay containing 0.01% neutral red in overlay medium, incubated at 37°C, and plaques were counted the next day. Plaque assays for influenza virus were done in MDCK cells (Tobita et al., 1975), and for VSV in BHK21 cells (Roth and Compans, 1980).

Radiolabeling of viral polypeptides

Confluent Vero cell monolayers in 35 mm dishes were washed twice with PBS and inoculated with IBV at a multiplicity of 0.5 pfu per cell. After incubation at 37°C for 2 h, the inoculum was removed, cells were refed with serum-free Eagle's minimal essential medium containing various concentrations of monensin and kept at 37°C. At 19 h postinfection, cells were treated for 5 h with 0.5 μg/ml of actinomycin D to reduce the background of cellular protein synthesis and then pulse-labeled for 1 h with 50 μCi/dish of [^{3}H]leucine in 0.2 ml of leucine-free Eagle's medium or 50 μCi/dish of [^{3}H]glucosamine in 0.2 ml of Eagle's medium. The ionophore was present at all times in the case of monensin-treated cells. At the end of the pulse, cells were washed 5 times with PBS and solubilized in sample reducing buffer (0.0625 M Tris-HCl, pH 6.8, containing 0.5% 2-mercaptoethanol, 10% glycerol and 2.3% SDS).

Polyacrylamide gel electrophoresis

Samples for SDS–polyacrylamide gel electrophoresis (SDS–PAGE) were boiled for 2 min prior to loading. Electrophoresis was done on 10% polyacrylamide slab gels (Laemmli, 1970) for 16–18 h at a constant current of 9 mA per slab gel. At the end of the run, gels were fixed for 30 min in 10% acetic acid/40% methanol in distilled water, and processed for fluorography (Bonner and Laskey, 1974). Dried gels were exposed on Kodak X-Omat AR films at −70°C.

Electron microscopy

Cells were fixed in situ with 1% glutaraldehyde in PBS for 30 min, followed by post-fixation with 1% osmium tetroxide for 40 min at 4°C. The cells were then

further processed as detailed previously (Alonso and Compans, 1981). Thin sections were stained with uranyl acetate and lead citrate, and examined in a Philips 301 electron microscope.

Chemicals and isotopes

Monensin was obtained from Calbiochem-Behring Corp. (La Jolla, Calif.), and α-amanitin was from Sigma Chemical Co. (St. Louis, Mo). L-[4,5-^{3}H (N)]leucine (sp. act. 59.8 Ci/mmol) was purchased from New England Nuclear (Boston, Mass.) and D-[6-^{3}H]-glucosamine (sp. act. 26.8 Ci/mmol) was purchased from Amersham (Arlington Heights, Ill.).

Results

Replication of IBV in Vero cells

The eclipse phase for IBV in Vero cells was found to be from 4 to 8 h, followed by a progressive production of virions. Release of virions commenced about 8 h postinfection, and maximum titers of about 10^6 pfu/ml were obtained at 30–45 h postinfection. Syncytium formation was first observed at 15 h after virus infection, with from 3 to 5 nuclei per cell. The syncytia then enlarged rapidly to 10–20 nuclei by 18 h and to 30–40 nuclei by 22 h postinfection (data not shown). The syncytia detached from the substrate as infection progressed.

The fungal toxin α-amanitin inhibits the function of cellular RNA polymerases (Roeder, 1976), and has been shown to block the replication of influenza virus but not of VSV (Mahy et al., 1972; Evans and Simpson, 1980). It has been reported that replication of IBV in BHK21 cells was blocked when the cells were enucleated, irradiated with ultraviolet light prior to infection, or treated with α-amanitin during virus growth, suggesting a requirement for an intact cell nucleus as well as one or more host transcriptional activities for productive infection (Evans and Simpson, 1980). We observed that a concentration of 20 μg/ml of α-amanitin inhibited influenza virus replication in Vero cells by over 100-fold as compared to control yields, whereas VSV was insensitive to the drug at this concentration (Fig. 1). At this concentration of α-amanitin, there was no significant inhibition in the yield of IBV; less than a 2-fold reduction in yield of released IBV virions was observed under conditions which caused a drastic reduction in influenza virus infectivity titers. IBV replication in Vero cells was also found to be much less sensitive to actinomycin D than was replication of influenza virus in these cells (not shown). At a concentration of 2 μg/ml of actinomycin D, we observed a 1000-fold reduction in yields of infectious influenza virus whereas infectivity titers of released IBV virions were reduced by less than 10-fold.

Virus maturation in Vero cells

Thin sections of IBV-infected Vero cells usually showed mature virus particles with diameters ranging from 60 to 100 nm in dilated cisternae of the RER as well as in smooth-walled vesicles (Fig. 2A). In some cells, cross-sections of IBV particles

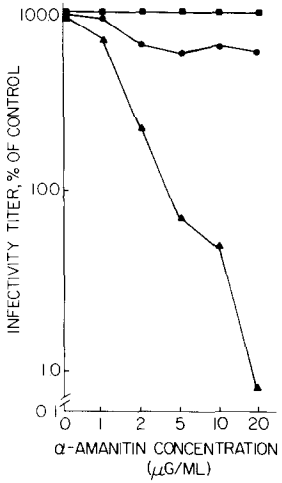

Fig. 1. Yields of IBV, influenza virus and VSV in α-amanitin-treated cells. Confluent Vero cell monolayers were infected with 0.5 pfu per cell of IBV, or 2 pfu per cell of influenza virus or VSV. Following virus adsorption at 37°C, the infected cells were incubated either with regular DMEM or medium containing various concentrations of α-amanitin. The 24 h virus yields were determined by plaque assays. Infectivity titers of released IBV (●); influenza virus (▲); VSV (■). The control (100%) infectivity titers were 2.8×10^5 pfu/ml (IBV); 4.7×10^7 pfu/ml (influenza virus); 2.5×10^9 pfu/ml (VSV).

were also observed free in the cytoplasm of infected cells, i.e. not contained within RER membranes or cytoplasmic vesicles (Fig. 2B). Virions were observed to mature by budding at intracellular membranes of the RER as seen in Fig. 2C; such budding occurs by formation of crescents, or areas of the membrane which bulged toward the lumen of the RER on which a layer of dense material was apposed. Usually, distinct striations were observed within the virus particles as shown in the leftmost inset of Fig. 2C. These striations have a diameter of 2–3 nm, which is similar to that of helical ribonucleoprotein complexes reported by others (Davies et al., 1981). In some profiles, such as the particle shown in the right inset of Fig. 2C, virions were found to contain from 12 to 14 electron-dense globular structures of similar diameter, just within the perimeter of the envelope; these structures probably represent the helical ribonucleoprotein complexes in cross-section. These profiles suggest that the ribonucleoprotein is closely associated with the viral envelope.

In addition to typical IBV particles, two other structures were observed at later times postinfection (Fig. 3). Enveloped ribosome-containing particles, with diameters ranging from 50 to 200 nm, were observed in large numbers in perinuclear areas. These ribosome-containing structures were absent in uninfected Vero cells or in IBV-infected cells at early stages of infection; they appeared to be derived from vesiculation of the RER membrane, possibly as a result of overproduction of viral membrane proteins which may accumulate at this site. Many of the ribosome-containing particles appeared to show a discontinuity in their envelope, also suggesting that they may result from an aberrant budding process. In addition, smooth-walled vesicles, which appeared empty in cross-section, were found in adjacent regions of

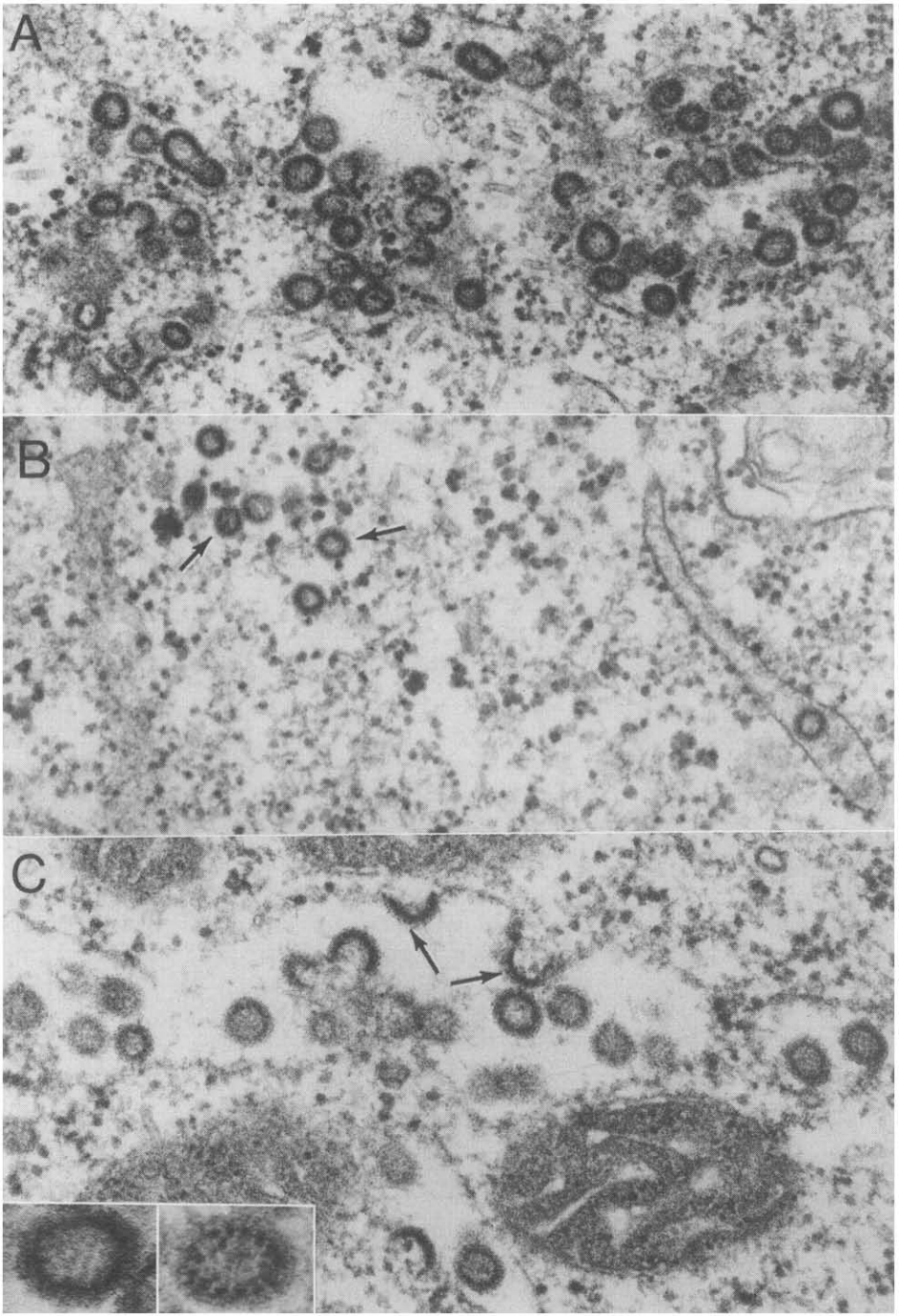

Fig. 2. Thin sections of Vero cells infected with the Beaudette strain of IBV. (A) An infected cell at 24 h postinfection showing an accumulation of IBV particles contained within dilated cisternae of the RER (×67000). (B) IBV particles free in the cytoplasm, i.e. not contained within the RER lumen or in vesicles (arrows). In contrast, an IBV virion found within the RER can also be seen. (× 63000). (C) An IBV-infected Vero cell at 30 h postinfection showing virions budding at the membranes of the RER (arrows). (×88000). Insets show high magnification views of IBV particles showing internal striations or electron-dense globular structures within the perimeter of the envelope. (×160000).

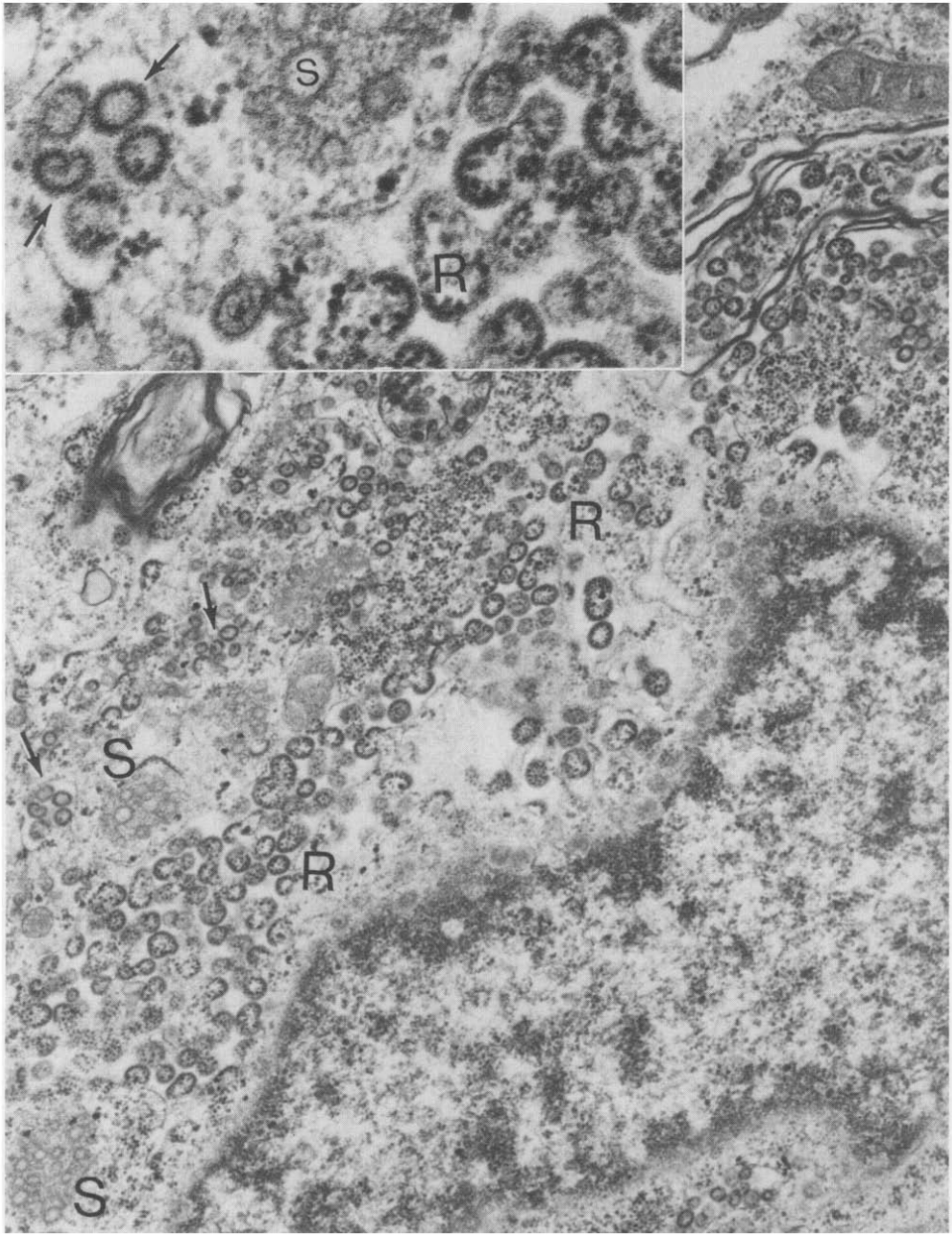

Fig. 3. Thin section of a Vero cell infected with IBV at 24 h postinfection. The arrows point to a group of typical IBV particles which are enclosed in a vesicle. In the perinuclear region are numerous enveloped particles which appear to contain ribosomes (R); they are slightly larger in diameter than typical IBV virions. A third type of structure consists of smooth vesicles (S) surrounded by electron-dense filamentous elements ($\times 32000$). Inset shows a higher magnification view of the structures described. ($\times 100000$).

the cytoplasm. These structures were observed in clusters, and were surrounded by electron-dense filamentous structures (Fig. 3, inset).

Effect of monensin on IBV replication in Vero cells

Monensin, a monovalent ionophore, has been reported to block the appearance of membrane glycoproteins on the cell surface as well as the release of secretory glycoproteins in a variety of eukaryotic cells (reviewed by Tartakoff, 1983). Since evidence has been obtained that monensin inhibits the exit of membrane glycoproteins from the Golgi complex (Tartakoff and Vassalli, 1977, 1978), it was of interest to compare the effects of monensin on the replication of viruses known to mature on the cell surface, e.g. VSV, with that of IBV, which forms by budding at intracellular membranes. As shown in Fig. 4, VSV yields in Vero cells were reduced by about 2-fold at a 10^{-6} M concentration of monensin, and by about 100-fold as compared to controls at 10^{-5} M, the highest concentration tested. Release of infectious IBV was more sensitive to the ionophore, with greater than a 10-fold decrease in virus yield at 10^{-6} M, and a reduction of over 1000-fold at 10^{-5} M monensin. The titers of cell-associated IBV virions, obtained by one cycle of freeze-thawing, were reduced slightly at 10^{-6} M monensin concentration; at 10^{-5} M monensin, however, only low levels of cell-associated IBV virions were detected.

To further investigate the effects of monensin on assembly of IBV virions, we examined thin sections of IBV-infected Vero cells in the presence of a 10^{-6} M (Fig. 5A) or 10^{-5} M (Fig. 5B) concentration of the ionophore. Dilated cytoplasmic

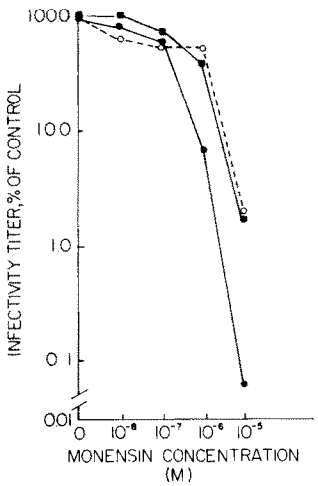

Fig. 4. Effect of monensin on yields of IBV and VSV from Vero cells. Monensin was added postadsorption to confluent Vero cell monolayers infected with 0.5 pfu per cell of IBV, or 2 pfu per cell of VSV. Culture fluids were harvested 24 h postinfection and infectivity titers were determined by plaque assays. In the case of IBV, yields of both released and cell-associated virions, obtained after one cycle of freeze-thawing, were measured. ●, released IBV titers; ○, cell-associated IBV titers; ■, VSV infectivity titers. The control (100%) titer was 4.5×10^5 pfu/ml for released IBV, 1.1×10^5 pfu/ml for cell-associated IBV, and 2.7×10^9 pfu/ml for VSV.

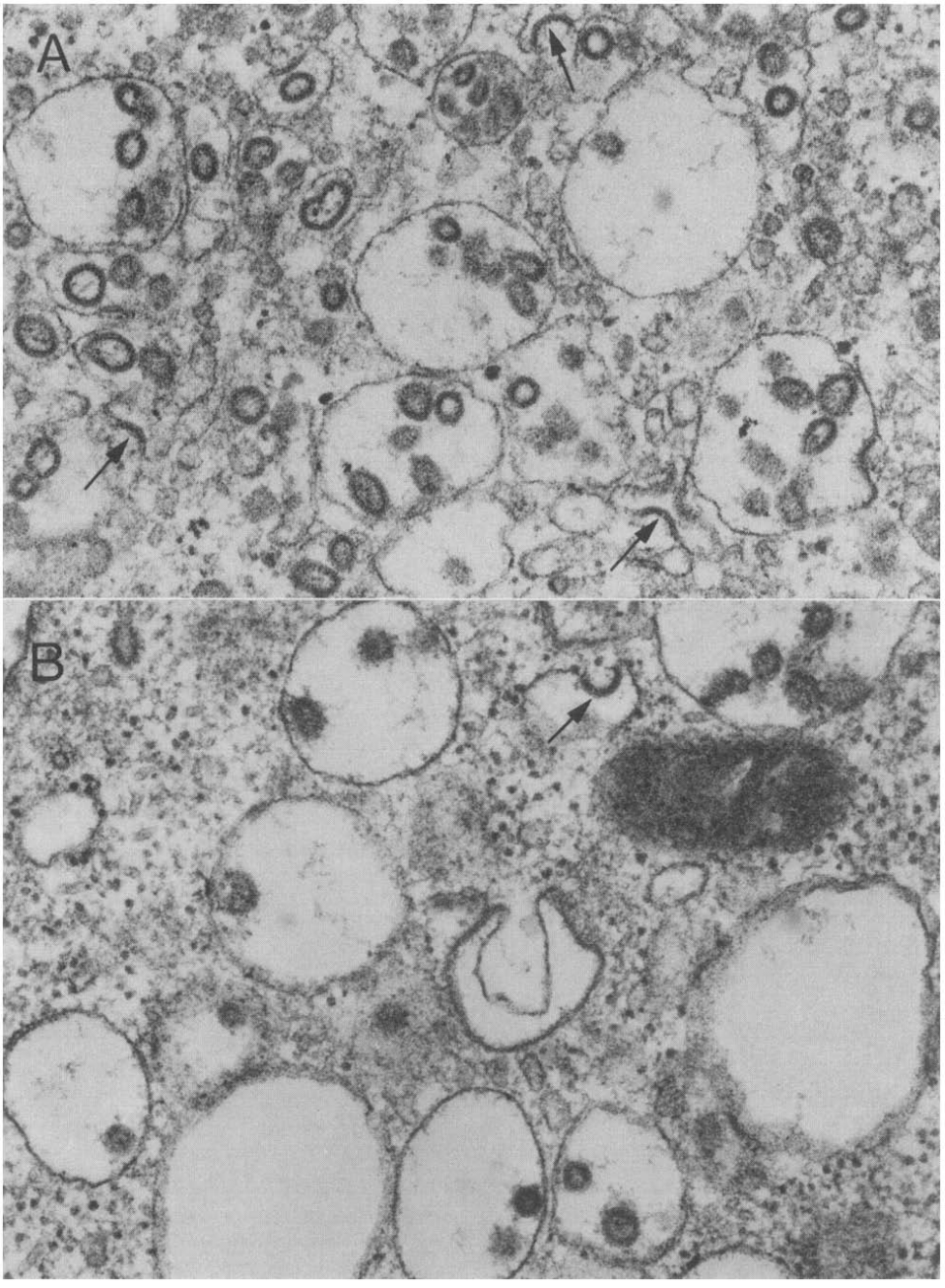

Fig. 5. Thin sections of Vero cells at 24 h postinfection with IBV in the presence of 10^{-6} M (A) or 10^{-5} M (B) monensin. IBV particles are located within dilated cytoplasmic vesicles. The arrows point to budding virus particles. ($\times 70000$).

vesicles were observed which contained IBV particles; however, the concentration of particles was not increased when compared to controls, and was greatly reduced in the case of cells treated with 10^{-5} M monensin. The vesicles, which are presumed to be of Golgi origin, are similar to structures previously described in monensin-treated cells (Tartakoff and Vassalli, 1977, 1978; Johnson and Schlesinger, 1980), and are markedly dilated when compared to smooth cytoplasmic vesicles found in untreated IBV-infected Vero cells. These results indicate that assembly of infectious IBV is significantly inhibited by monensin; reductions in yields of released virus are not merely a result of intracellular accumulation of virions.

Viral protein synthesis in monensin-treated cells

To determine the effect of monensin on the synthesis of viral proteins, [^{3}H]leucine-labeled IBV-infected Vero cell lysates obtained in the presence of various concentrations of the ionophore were analyzed by SDS–PAGE. Three major virus-specific polypeptides with estimated mol. wts. of 170000, 52000 and 24000 were clearly resolved in untreated IBV-infected cell lysates (Fig. 6, lane b); addi-

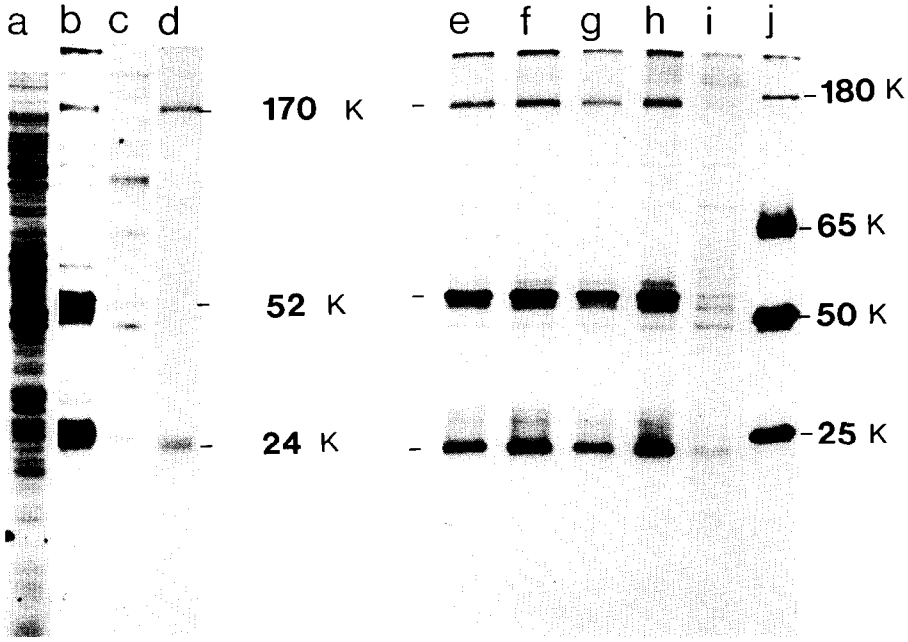

Fig. 6. Viral protein synthesis in untreated or monensin-treated Vero cells. Cells were radiolabeled for 1 h with either [^{3}H]leucine (lanes a and b; e to i) or [^{3}H]glucosamine (lanes c and d) at 24 h postinfection as described in Materials and Methods and viral polypeptides were analyzed by SDS–PAGE. Lanes a and c, mock-infected; b and d, IBV-infected. Equal volumes of cell lysate containing approximately equal cpm were loaded in lanes e to i; in the case of lane i, the volume was doubled to load equivalent cpm. Lane e, IBV-infected, untreated; f, 10^{-8} M monensin; g, 10^{-7} M monensin; h, 10^{-6} M monensin; i, 10^{-5} M monensin; j, VSV viral proteins used as molecular weight standards.

tional minor bands were present, but corresponded to polypeptides present in mock-infected cells. Two of these polypeptides (170000 and 24000 daltons) were found to be glycosylated (Fig. 6, lane d), and are designated gp170 and gp24. The three virus-specific polypeptides were also detected in infected cells treated with various concentrations of the ionophore (Fig. 6, lanes e to i). There were no significant changes observed in the amounts of electrophoretic mobilities of any of these polypeptides at concentrations of monensin up to 10^{-6} M, where infectious virus yields were reduced by over 10-fold. This supports the conclusion that monensin inhibits the formation of infectious IBV particles under conditions where no effect on viral protein synthesis is observed. Only at the highest concentration of monensin tested (10^{-5} M) was there a significant decrease in viral protein synthesis. This concentration of the drug, however, was found to inhibit protein synthesis by more than 2-fold in uninfected Vero cells (not shown).

Discussion

We have propagated IBV in a continuous cell line, Vero, which is of African green monkey kidney origin. Previous reports (Coria and Ritchie, 1973; Cunningham et al., 1972) described the serial passage of IBV in Vero cells after initial adaptation in embryonated eggs and chicken embryo kidney cells (CEK), followed by passages in suckling mouse brain; however, the maximum infectious virus yield reported was significantly lower than that observed in the present study. We have also investigated aspects of the replication process of IBV in Vero cells using α-amanitin, a fungal toxin which inhibits DNA-dependent RNA polymerase II, and actinomycin D, which binds to DNA and impedes the movement of RNA polymerase (Roeder, 1976). Under experimental conditions and drug concentrations which significantly inhibited growth in Vero cells of influenza virus, but not of VSV, we have observed that IBV replication in Vero cells is relatively resistant to α-amanitin, as well as to low concentrations of actinomycin D, indicating that host cell RNA polymerase activity is not required for growth of IBV. In previous reports on the sensitivity of coronavirus replication to these two drugs, human coronavirus 229E (Kennedy and Johnson-Lussenberg, 1979) and IBV propagated in BHK21 cells (Evans and Simpson, 1980) were reported to be sensitive to actinomycin D, and IBV was also reported to be sensitive to α-amanitin (Evans and Simpson, 1980). However, there was no reduction observed in the yield of infectious IBV from actinomycin D-treated CEK cells (Stern and Kennedy, 1980). Replication of mouse hepatitis virus was also reported to be insensitive to actinomycin D (Brayton et al., 1981; Wilhelmsen et al., 1981; Mahy et al., 1983) and to α-amanitin (Mahy et al., 1983), indicating that DNA-directed RNA synthesis does not play a significant role in murine coronavirus replication.

Examination of thin sections of IBV-infected Vero cells showed mature virus particles located in dilated cisternae of the RER as well as in smooth cytoplasmic vesicles. This observation is consistent with other studies on coronavirus morphogenesis. Coronaviruses mature by budding from the intracellular membranes of the

RER and migrate through the Golgi apparatus, and are transported to the plasma membrane via Golgi-derived vesicles; virions are then presumably released from intact cells by fusion of these vesicles with the plasma membrane (Robb and Bond, 1979; Holmes et al., 1981). The present finding of some IBV particles apparently free in the cytoplasm is unusual; possibly, this results from disruption of intracellular vesicles containing virus particles. A striking feature of IBV-infected Vero cells at late stages in infection was the presence of numerous enveloped particles containing ribosomes. We suggest that these structures are derived from infoldings of the RER as a result of modification by viral membrane proteins.

The radiolabeling protocol used in the present study revealed three major viral polypeptides, including two glycoproteins, which were readily detected above the host cell background. In a previous study of IBV-infected CEK cells, a more complex pattern of polypeptides was reported, with nine polypeptide species detected in immune precipitates (Stern and Sefton, 1982a). However, most of these were species produced by posttranslational modifications including proteolytic cleavage of a precursor designated gp155, or differences in extent of glycosylation of a polypeptide designated p23 (Stern and Sefton, 1982b). It is likely that the gp170 polypeptide we observed in Vero cells corresponds to gp 155 detected in CEK cells, and that gp24 corresponds to the p23-related polypeptides. Neither proteolytic cleavage products of the larger glycoprotein nor differentially-glycosylated forms of the smaller glycoprotein were detected in significant amounts in IBV-infected Vero cells, although some heterogeneity was evident in the gp24 component. These results suggest that polypeptide synthesis in IBV-infected Vero cells may resemble patterns observed with mammalian coronaviruses (Sturman, 1977; Siddell et al., 1982); additional viral polypeptides may be present at low levels, but were not resolved. Analysis of the glycosylation process of IBV glycoproteins in Vero cells has indicated that gp170 and gp24 both possess N-linked oligosaccharides (Y. Matsuoka, unpublished), as has been observed for IBV glycoproteins in avian cells (Stern and Sefton, 1982b; Cavanagh, 1983).

Monovalent ionophores such as monensin have been shown to inhibit the intracellular transport of both membrane and secretory glycoproteins from their site of synthesis in the RER to the plasma membranes of eukaryotic cells (reviewed by Tartakoff, 1983), with a block in transport occurring at the level of the Golgi complex. Since IBV was observed to bud at intracellular membranes of the RER, we compared the effects of monensin on the assembly of IBV with its effect on other enveloped viruses that form at the cell surface. We observed that production of infectious IBV particles was inhibited significantly at high concentrations of ionophore. The inhibition of IBV replication by monensin occurred under conditions where no effect on viral protein synthesis was observed. Examination of thin sections of monensin-treated cells showed mature IBV particles located in dilated cytoplasmic vesicles, which are probably also derived from the Golgi membranes (Alonso and Compans, 1981; Tartakoff and Vassalli, 1977, 1978). Since the inhibition of IBV release was not paralleled by an accumulation of cell-associated virions, monensin apparently did not merely block the exocytosis of infectious particles. In a previous study of 17C11 cells infected with murine coronavirus, however, virus

budding was apparently not inhibited by monensin, and virions were found to accumulate in large amounts within the RER (Niemann et al., 1982). The E1 glycoprotein of murine coronaviruses possesses O-linked oligosaccharides which are added post-translation, and glycosylation of this polypeptide was completely blocked in monensin-treated cells (Niemann et al., 1982). In contrast, we found that the electrophoretic mobilities of IBV glycoproteins were not altered in monensin-treated cells, indicating that the incorporation of N-linked oligosaccharides continues normally in these glycoproteins. These results indicate that significant differences exist in the glycoprotein processing of avian vs. mammalian coronaviruses.

Several possible mechanisms can be envisioned for inhibition of IBV assembly by monensin. Although most of the oligosaccharides linked to IBV glycoproteins were reported to be of the N-linked high mannose type, some N-linked complex oligosaccharides were also present (Stern and Sefton, 1982b). It has not been determined whether the formation of such complex chains occurs after virus assembly, as completed virions pass through the Golgi complex en route to the cell surface, or whether some viral glycoproteins pass through the Golgi complex, and are recycled to the RER prior to virus maturation. The latter process would be expected to be sensitive to the ionophore. Alternatively, the changes in intracellular pH and ion concentrations induced by monensin treatment of host cells may have a direct effect on virus assembly.

Acknowledgements

We thank L.R. Melsen for assistance with electron microscopy, and Vivian Brown and Tawana Burts for technical assistance.

This research was supported by grant PCM 80-06498 from the National Science Foundation, CA 13148 and CA 18611 from the National Cancer Institute and AI 12680 from the National Institute of Allergy and Infectious Diseases. F.V. Alonso-Caplen was partially supported by Institutional Research Service Award AI 07150 from the National Institute of Allergy and Infectious Diseases.

References

Alonso, F.V. and Compans, R.W. (1981) Differential effects of monensin on enveloped viruses that form at distinct plasma membrane domains. J. Cell Biol. 89, 700–705.

Alonso-Caplen, F.V. and Compans, R.W. (1983) Modulation of glycosylation and transport of viral membrane glycoproteins by a sodium ionophore. J. Cell Biol. 97, 659–668.

Becker, W.B., McIntosh, K., Dees, J.H. and Chanock, R.M. (1967) Morphogenesis of avian infectious bronchitis virus and a related human virus (strain 229E). J. Virol. 1, 1019–1027.

Bonner, W.M. and Laskey, R.A. (1974) A film detection method of tritium-labeled proteins and nucleic acids in polyacrylamide gels. Eur. J. Biochem. 46, 83–88.

Brayton, P.R., Ganges, R.G. and Stohlman, S.A. (1981) Host cell nuclear function and murine hepatitis virus replication. J. Gen. Virol. 56, 457–460.

Cavanagh, D. (1983) Coronavirus IBV glycopolypeptides: size of their polypeptide moieties and nature of their oligosaccharides. J. Gen. Virol. 64, 1187–1192.

Choppin, P. W. (1969) Replication of influenza virus in a continuous cell line: High yield of infective virus from cells inoculated at high multiplicity. Virology 38, 130–134.

Coria, M.F. and Ritchie, A.E. (1973) Serial passage of 3 strains of avian infectious bronchitis virus in African Green monkey kidney cells (Vero). Avian Dis. 17, 697–704.

Cunningham, C.H., Spring, M.P. and Nazerian, K. (1972) Replication of avian infectious bronchitis virus in African Green monkey kidney cell line Vero. J. Gen. Virol. 16, 423–427.

Davies, H.A., Dourmashkin, R.R. and MacNaughton, M.T. (1981) Ribonucleoprotein of avian infectious bronchitis virus. J. Gen. Virol. 53, 67–74.

Evans, M.R. and Simpson, R.W. (1980) The coronavirus avian infectious bronchitis virus requires the cell nucleus and host transcriptional factors. Virology 105, 582–591.

Holmes, K.V. and Choppin, P.W. (1966) On the role of the response of the cell membrane in determining virus virulence. Contrasting effects of the parainfluenza SV5 in two cell types. J. Exp. Med. 124, 501–520.

Holmes, K.V., Doller, E.W. and Sturman, L.S. (1981) Tunicamycin resistant glycosylation of a coronavirus glycoprotein: demonstration of a novel type of viral glycoprotein. Virology 115, 334–344.

Johnson, D.C. and Schlesinger, M.J. (1980) Vesicular stomatitis virus and Sindbis virus glycoprotein transport to the cell surface is inhibited by ionophores. Virology 103, 407–424.

Johnson, D.C. and Spear, P.G. (1982) Monensin inhibits the processing of herpes simplex virus glycoproteins, their transport to the cell surface, and the egress of virions from infected cells. J. Virol. 43, 1102–1112.

Kennedy, D.A. and Johnson-Lussenberg, C.M. (1979) Inhibition of coronavirus 229E replication by actinomycin D. J. Virol. 29, 401 404.

Laemmli, U.L. (1970) Cleavage of structural proteins during the assembly of the head of bacteriophage T4. Nature (London) 227, 680–682.

Ledger, P.W., Uchida, N. and Tanzer, M.L. (1980) Immunocytochemical localization of procollagen and fibronectin in human fibroblasts: effects of the monovalent ionophore, monensin. J. Cell Biol. 87, 663–671.

Madoff, D.H. and Lenard, J. (1982) A membrane glycoprotein that accumulates intracellularly: cellular processing of the large glycoprotein of LaCrosse virus. Cell 28, 821–829.

Mahy, B.W.J., Hastie, N.D. and Armstrong, S.J. (1972) Inhibition of influenza virus replication by α-amanitin: mode of action. Proc. Natl. Acad. Sci. U.S.A. 69, 1421–1424.

Mahy, B.W.J., Siddell, S., Wege, H. and ter Meulen, V. (1983) RNA-dependent RNA polymerase activity in murine coronavirus-infected cells. J. Gen. Virol. 64, 103–111.

Niemann, H., Boschek, B., Evans, D., Rosing, M., Tamura, I. and Klenk, H.-D. (1982) Posttranslational glycosylation of coronavirus glycoprotein E1: inhibition by monensin. EMBO J. 1, 1499–1504.

Robb, J.A. and Bond, C.W. (1979) Coronaviridae. In: Comprehensive Virology, Vol. 14 (Fraenkel-Conrat, H. and Wagner, R.R., eds.), pp. 193–247. Plenum Press, New York.

Roeder, R.G. (1976) Eukaryotic nuclear RNA polymerases. In: RNA Polymerase (Losik, R. and Chamberlin, N., eds.), pp. 285–329. Cold Spring Harbor Laboratory, Cold Spring Harbor, N.Y.

Roth, M.G. and Compans, R.W. (1980) Antibody-resistant spread of vesicular stomatitis virus infection in cell lines of epithelial origin. J. Virol. 35, 547–550.

Schochetman, G., Stevens, R.H. and Simpson, R.W. (1977) Presence of infectious polyadenylated RNA in the coronavirus avian bronchitis virus. Virology 77, 772–782.

Siddell, S., Wege, H. and ter Meulen, V. (1982) The structure and replication of coronaviruses. Curr. Top. Microbiol. Immunol. 99, 131–163.

Siddell, S., Wege, H. and ter Meulen, V. (1983) The biology of coronaviruses. J. Gen. Virol. 64, 761–776.

Srinivas, R.V., Melsen, L.R. and Compans, R.W. (1982) Effects of monensin on morphogenesis and infectivity of Friend murine leukemia virus. J. Virol. 42, 1067–1075.

Stern, D.F. and Kennedy, S.I.T. (1980) Coronavirus multiplication strategy. I. Identification and characterization of virus-specified RNA. J. Virol. 34, 665–674.

Stern, D.F. and Sefton, B.M. (1982a) Coronavirus proteins: biogenesis of avian infectious bronchitis virus virion proteins. J. Virol. 44, 794–803.

Stern, D.F. and Sefton, B.M. (1982b) Coronavirus proteins: structure and function of the oligosaccharides of the avian infectious bronchitis virus glycoproteins. J. Virol. 44, 804–812.

Sturman, L.S. (1977) Characterization of a coronavirus I. Structural proteins: effects of preparative conditions on the migration of protein in polyacrylamide gels. Virology 77, 637–649.

Tajiri, K., Uchida, N. and Tanzer, M.L. (1980) Undersulfated proteoglycans are secreted by cultured chondrocytes in the presence of the ionophore monensin. J. Biol. Chem. 365, 6036–6039.

Tartakoff, A.M. (1983) Perturbation of vesicular traffic with the carboxylic ionophore monensin. Cell 32, 1026–1028.

Tartakoff, A.M. and Vassalli, P. (1977) Plasma cell immunoglobulin secretion: arrest is accompanied by alterations of the Golgi complex. J. Exp. Med. 146, 1332–1345.

Tartakoff, A.M. and Vassalli, P. (1978) Comparative studies of intracellular transport of secretory proteins. J. Cell Biol. 79, 694–707.

Tobita, K., Sugiura, A., Enomoto, E. and Furuyama, M. (1975) Plaque assay and primary isolation of influenza A virus in an established line of canine kidney cells (MDCK) in the presence of trypsin. Med. Microbiol. Immunol. 162, 9–14.

Wilhelmsen, K.C., Lebowitz, J.L., Bond, C.W. and Robb, J.A. (1981) The replication of murine coronaviruses in enucleated cells. Virology 110, 225–230.

(Manuscript received 10 November 1983)